

University of Texas Rio Grande Valley

ScholarWorks @ UTRGV

Physics and Astronomy Faculty Publications
and Presentations

College of Sciences

2020

A simple graphical method for calculating the standing wave frequencies on a rectangular membrane

Joseph D. Romano

The University of Texas Rio Grande Valley

Richard H. Price

Follow this and additional works at: https://scholarworks.utrgv.edu/pa_fac



Part of the [Astrophysics and Astronomy Commons](#), and the [Physics Commons](#)

Recommended Citation

Romano, Joseph D., and Richard H. Price. "A simple graphical method for calculating the standing wave frequencies on a rectangular membrane." *American Journal of Physics* 88, no. 8 (2020): 605-611. <https://doi.org/10.1119/10.0001299>

This Article is brought to you for free and open access by the College of Sciences at ScholarWorks @ UTRGV. It has been accepted for inclusion in Physics and Astronomy Faculty Publications and Presentations by an authorized administrator of ScholarWorks @ UTRGV. For more information, please contact justin.white@utrgv.edu, william.flores01@utrgv.edu.

PAPERS | AUGUST 01 2020

A simple graphical method for calculating the standing wave frequencies on a rectangular membrane

Joseph D. Romano; Richard H. Price



Am. J. Phys. 88, 605–611 (2020)

<https://doi.org/10.1119/10.0001299>



View
Online



Export
Citation

CrossMark



A simple graphical method for calculating the standing wave frequencies on a rectangular membrane

Joseph D. Romano^{a)}

Department of Physics and Astronomy, Texas Tech University, Box 41051, Lubbock, Texas 79409-1051

Richard H. Price^{b)}

Department of Physics, Massachusetts Institute of Technology, Cambridge, Massachusetts 02139

(Received 4 March 2020; accepted 25 April 2020)

In introductory physics courses, simple arguments based on traveling waves on a string are used to relate the frequency of standing waves to boundary conditions, e.g., the fixed ends of the string. Here, we extend that approach to two-dimensional waves such as the oscillations of a rectangular membrane with edges fixed at the boundary. This results in a graphical method that uses only simple geometry and is suitable for explaining two-dimensional standing-wave oscillations to non-science majors, e.g., in a physics of sound and music class. © 2020 American Association of Physics Teachers.

<https://doi.org/10.1119/10.0001299>

I. INTRODUCTION

Standing-wave oscillations on a string are a fundamental component of any course on the physics of sound and music. Work can be found in the pedagogical literature on apparatuses,¹⁻⁴ demonstrations,⁵⁻⁷ student laboratories and projects,^{8,9} and principles.^{10,11} Standing waves are the “building blocks” from which *any* periodic vibration (e.g., that of a plucked guitar string¹²⁻¹⁴) can be constructed (thanks to Fourier’s theorem). The frequencies of the standing-wave oscillations for a string of length L fixed at both ends are given by

$$f_n = n \frac{v}{2L}, \quad n = 1, 2, \dots, \quad (1)$$

where v is the velocity of the waves on the string. The fact that only a discrete set of frequencies (labeled by the harmonic number n) are allowed for the standing waves can be easily demonstrated in the classroom, e.g., using a mechanical vibrator with an adjustable driving frequency attached to one end of a string under tension. Another demonstration of the nature of the oscillations is the motion of the string if it is plucked or bowed. When the frequency content of this motion is studied with a spectrum analyzer one sees contributions from these special harmonic frequencies. Sounds that have large contributions from many harmonics are often perceived as having a “richer” tone than sounds that have contributions from only a few harmonics.

Typically, the standing wave frequencies (1) are derived from the fundamental relation

$$v = f\lambda \quad (2)$$

for a periodic wave with frequency f and wavelength λ , noting that only an integer number of half-wavelengths can fit on a string of length L fixed at both ends—i.e., $n\lambda/2 = L$ or

$$\lambda = 2L/n, \quad n = 1, 2, \dots \quad (3)$$

This restriction on λ in turn restricts the allowed frequencies $f = v/\lambda$ to the values given in (1).

This idea of starting with fixed boundary conditions and “fitting in” the waves can be generalized to higher dimensions. For example, for a two-dimensional rectangular

membrane with edge lengths L_x, L_y , fixed at the boundaries, one typically proceeds using separation of variables,^{15,16} assuming a product-form solution to the two-dimensional wave equation, and requiring that the solution vanish on the boundaries (see Appendix A for details). This restricts the form of the product solutions, ultimately leading to standing-wave oscillations with frequencies

$$f_{nm} = \frac{v}{2} \sqrt{\left(\frac{n}{L_x}\right)^2 + \left(\frac{m}{L_y}\right)^2}, \quad n, m = 1, 2, \dots, \quad (4)$$

where n, m label the oscillation mode. However, unfortunately, the mathematical steps in the standard approach leading to the above expression are not appropriate for an introductory physics course, especially for non-science majors.

So, here we present an alternative (mostly) graphical approach for obtaining the standing-wave frequencies on a rectangular membrane, which requires only algebra and some basic high-school geometry. We start in Sec. II by rederiving the standing-wave frequencies on a 1D string by superimposing oppositely directed traveling waves but in a slightly different way than usual. Rather than starting with the boundary conditions and “fitting” in the waves—an order of ideas that we may call the “boundary-first” approach—we will do it the other way around. That is, we start with the superposition of the traveling waves and point out that the resulting nodes are “opportunities” to introduce the boundary conditions. In other words, we first find the nodes and then introduce the fixed ends of a string—a “boundary-last” approach that will better serve the argument for the 2D membrane that we discuss in Secs. III and IV. For the 2D case, we first superimpose oppositely directed quasi-1D traveling waves to get quasi-1D standing waves and then superimpose those quasi-1D standing waves to get the final 2D standing-wave oscillations having fixed rectangular boundaries. We conclude in Sec. V with a brief discussion.

We relegate to the Appendixes more advanced mathematical details: a brief summary of the standard separation-of-variable approach for 2D rectangular membranes (Appendix A), a graphical version of the boundary-first approach (Appendix B), and a trigonometric proof that a superposition of oppositely directed traveling waves yields standing waves (Appendix C).

II. 1D STANDING WAVES AS COMBINATIONS OF TRAVELING WAVES

So, let us begin with the 1D case by considering traveling waves on an “infinite” string (more generally for a 1D wave with no boundaries). In this approach to the problem, the wavelength λ (or, equivalently by (2), the frequency f) of the waves can have an arbitrary specified value. The top curve in Fig. 1 shows such a traveling wave. Let us focus on a particular location on the first wave pattern, a point at which the deviation of the string (i.e., its displacement away from its equilibrium position) is zero. This point moves to the right. Immediately below that wave is a picture of another wave that has the same wavelength and same amplitude, but it travels to the left. There will be some point on this pattern at which the deviation is zero, and this point moves to the left. There will be some instant, let’s somewhat arbitrarily call it time $t = 0$, at which these two points line up, an event that is marked by the vertical dashed line in Fig. 1.

Now, let us combine the right- and left-moving waves into a single dynamical motion of the string. We do that by simply adding the deviations of the two waves away from equilibrium, taking into account the signs of the deviations. As time increases, the contribution from the right-moving wave will decrease, while that of the left-moving wave will increase at the same rate, so the deviation of the combined wave will remain zero; we call such a point a *node* in the combined wave. It is easy to see that there will be an infinity of such nodes, one at every half wavelength.

We show the result of combining the waves in the third panel from the top in Fig. 1, where we show the pattern of deviations for the combined wave not only at $t = 0$ (corresponding to the solid curve with the largest amplitude) but also at subsequent (and earlier) times. Since the nodes are permanent zeroes, the motion of the string between the nodes is that of just oscillating up and down, something that is called a “standing wave” (standing because it is not traveling, showing no preference for right or left).

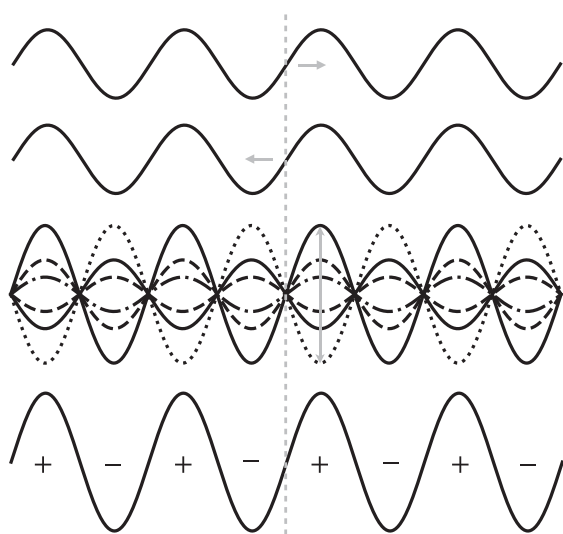


Fig. 1. The superposition of two oppositely directed traveling waves (top two panels) produces a standing wave (third panel), shown at multiple instants of time. Fourth panel: a snapshot of the standing wave at $t = 0$. Here, + and - denote positive and negative deviations of the string away from equilibrium.

In the bottom-most panel of Fig. 1, we show one more curve in order to introduce a new notation that will be very useful below. We show the standing-wave pattern at an instant of time, e.g., at the time we have chosen to call $t = 0$, and we denote with plus and minus the sign of the deviation for the half wavelengths between the nodes.

Finally, we raise the issue of boundary conditions, and note that the nodes of the standing-wave oscillations are locations at which we can place boundaries, e.g., mechanical fixtures for a string at which the string is fixed to have zero deviation, like the fixed ends of a guitar string.

It follows that the length L of a bounded string must be an integer number, call it n , of half wavelengths, so $L = n\lambda/2$. So, in this approach, where we start with traveling waves having an arbitrary wavelength (or frequency), it is the length of the bounded string that is constrained by the requirement that it have fixed ends. This is the boundary-last approach, but the real value of this argument requires that we turn it around in order to apply it to the physical situation we confront—one in which nature, or, e.g., a guitar maker, gives us the value of L , and we are to infer the wavelength (or frequency) of the traveling waves that combine to yield standing waves fixed at the boundaries. So, for the boundary-first approach, if there are n oscillating sections of the string (i.e., sections between nodes) and the string has fixed ends a distance L apart, then the frequency of the oscillation is $f = v/\lambda = nv/2L$, which is the same as (1).

III. 2D STANDING WAVES FROM ORTHOGONAL STANDING WAVES

We now consider an “infinite” 2D membrane, the 2D extension of our infinite 1D string. This could be something like a drumhead, except that—like the string initially considered above—it has no boundary. We start by realizing that there can be quasi-1D traveling waves in this membrane. These are waves (often called *plane waves*) that have straight-line wavefronts (e.g., lines of maximum deviation) and which propagate in a direction perpendicular to those wavefronts. The left panel of Fig. 2 shows such a wave. We can imagine this to be a quasi-1D wave traveling either toward or away from us. Or we can imagine it, as will we now do, to be a quasi-1D *standing* wave—the superposition of two quasi-1D traveling waves of equal wavelength and amplitude propagating in opposite directions.

We next add to our considerations a quasi 1D standing wave with its wavefronts oriented at 90° with respect to the first standing wave, as shown in the right panel in Fig. 2. This second, orthogonal standing wave has the same amplitude and wavelength (and hence frequency) as the first. We then combine the two quasi-1D standing waves just as we combined traveling waves, and we illustrate this superposition with the (relatively) simplified diagram of Fig. 3.

In this figure, the lines of nodes (i.e., lines of zero deviation) are indicated by solid and dotted lines; the solid black lines are the lines of zero deviation for the first standing wave and dotted red lines for the second. We use the plus/minus notation introduced for 1D waves, in which, at the moment of time we choose, a black plus sign indicates a positive deviation of the first standing wave and a black minus sign indicates a negative deviation. The red plus and minus signs do the same for the second standing wave. For definitiveness we choose an x, y coordinate system in which the origin lies in a positive deviation region of the first standing

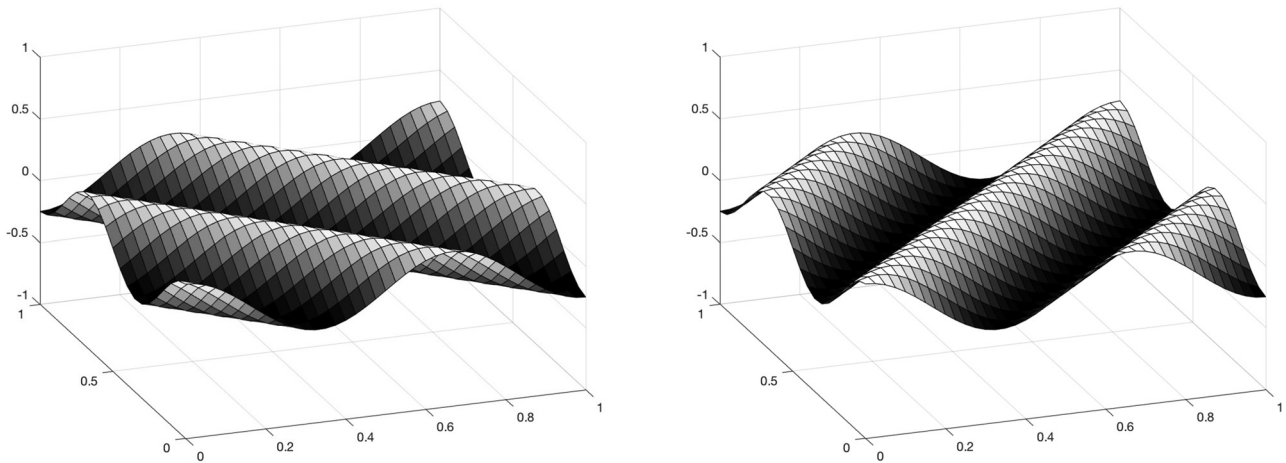


Fig. 2. Deviations from equilibrium of two orthogonal quasi-1D waves on a 2D membrane.

wave, halfway between two lines of nodes, and in a negative region of the second standing wave, halfway between two lines of nodes. We choose the orientation of our coordinate system so that the wavefronts (and hence the lines of nodes) lie at 45° to the coordinate axes, as shown in Fig. 3.

The blue dots in Fig. 3 mark the crossing of the lines of nodes. Let us focus for the moment on the points labeled 1 and 2, and let us consider the total deviation as we move from point 1 to point 2. As we proceed along this line, at the moment we discuss, the contribution from the first standing wave becomes more (and then less) negative at exactly the same rate that the contribution from the second standing wave becomes more (and then less) positive. The result is that the points along this dashed line are points of zero deviation. As time goes on, the changes in the contributions of both waves oscillate at the same frequency and always cancel; the dashed line going through points 1 and 2 is therefore a line on which the deviation is always zero—in other words, a *nodal line*.

Straightforward modifications of the above argument show that *all* the horizontal and vertical dashed blue lines

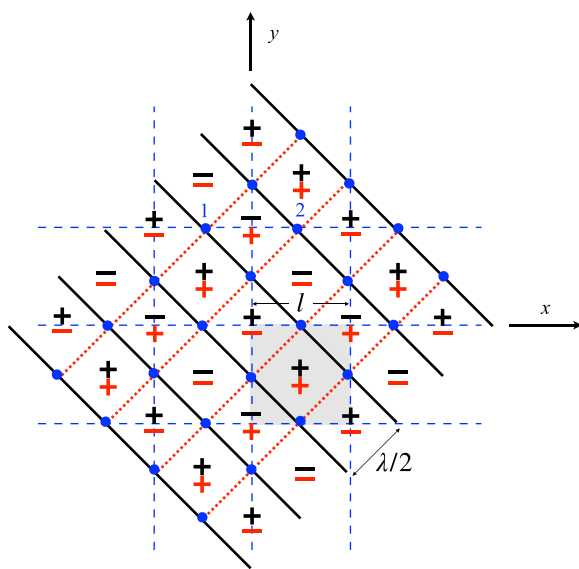


Fig. 3. Superposition of two quasi-1D standing waves oriented at 90° with respect to one another. The highlighted gray square is the region between a pair of neighboring vertical and horizontal nodal lines.

are zero-deviation lines. As in the case of imposing fixed ends on a guitar string, we now have an opportunity to impose fixed boundary conditions. We can choose any of the dashed blue lines as fixed positions of the edge of the 2D membrane.

So, just as we did for the 1D string, we now relate the frequency of the waves to the edge lengths of a 2D rectangular membrane that will be fixed at the boundaries. We first note that the region between a pair of neighboring vertical and horizontal dashed blue lines is simply a square (see the highlighted gray square in Fig. 3). This is a consequence of the wavefronts of the two quasi-1D standing waves being at right angles to one another. The length of a side of this square, which we will denote by l , is fixed by the wavelength λ . From Fig. 3, we see that l is $\sqrt{2}$ times $\lambda/2$, so $l = \lambda/\sqrt{2}$. However, we are not limited to choosing a square; we can choose any of the dashed blue lines in Fig. 3 as boundaries. Thus, the edge lengths L_x and L_y for a rectangular membrane with fixed boundaries must be integer multiples of l , so $L_x = n\lambda/\sqrt{2}$ and $L_y = m\lambda/\sqrt{2}$ for $n, m = 1, 2, \dots$. As before, we will apply these relations to the physical situation where the edge lengths L_x, L_y are given, and we are to infer the frequency of the standing waves. So, we invert these equations for the wavelength, $\sqrt{2}/\lambda = n/L_x = m/L_y$, and combine these last two expressions for $\sqrt{2}/\lambda$ by squaring and adding. The frequency is

$$f = \frac{v}{\lambda} = \frac{v}{2} \sqrt{\left(\frac{n}{L_x}\right)^2 + \left(\frac{m}{L_y}\right)^2}, \quad (5)$$

which agrees with (4) for the special geometry of orthogonal quasi-1D standing waves.

IV. GENERAL CASE: 2D STANDING WAVES FROM NON-ORTHOGONAL STANDING WAVES

To generalize the above construction, we start with quasi-1D traveling waves again having an arbitrary specified wavelength λ but not orthogonal to one another. For definiteness, we impose an x, y coordinate system and choose a propagation direction that has a slope of $2/3$ —i.e., a point on the wave advances two units in the y direction for every three units in the x direction. The second propagation direction is chosen to be symmetric about the x axis with respect to the

first. These directions and the choice of x, y coordinates are shown in the left panel of Fig. 4.

We now superimpose traveling waves having the same amplitude and wavelength as these but with opposite directions, so that we produce quasi-1D standing waves with non-orthogonal wavefronts. For the $\pm 2/3$ propagation directions that we have chosen, the wavefronts are shown in the right panel of Fig. 4, which is the equivalent of Fig. 3. All the arguments we applied to Fig. 3 now apply to Fig. 4, and we find the new lines of zero deviation, shown, as in Fig. 3, by dashed blue lines. Again, these dashed blue lines represent the locations at which zero deviation (i.e., fixed) boundaries might be imposed.

As we did earlier, we now want to find the relationship between the geometry of the boundaries and the frequencies of the 2D standing waves. This will require some high school geometry. (You knew it would be useful some day; today is the day.) We first note from the right panel of Fig. 4 that the aspect ratio of the rectangular region enclosed by neighboring vertical and horizontal boundaries is 2:3. This is a consequence of the propagation directions of the non-orthogonal quasi-1D traveling waves. To determine the overall length scale of this region, which we denote by l , we focus attention on the space between two wavefronts and add some lines to support the analysis. (See the highlighted gray triangle in Fig. 4 and an enlarged version of it in Fig. 5 for details.) One of those lines shows the distance, $\lambda/2$, between two zero deviation wavefronts of the quasi-1D standing wave. The other lines serve to show the slope of the wavefronts. To discuss the triangles we have just formed, we label vertices with Greek letters.

We can now see that $\alpha\beta\gamma$ and $\alpha\delta\beta$ are similar right triangles, so $\lambda/2$ divided by $2l$ is equal to $3l$ divided by the length $\sqrt{(2l)^2 + (3l)^2}$ of line segment $\alpha\gamma$, so

$$\frac{(\lambda/2)}{2l} = \frac{3l}{\sqrt{(2l)^2 + (3l)^2}} \iff \frac{1}{(\lambda/2)} = \sqrt{\left(\frac{1}{2l}\right)^2 + \left(\frac{1}{3l}\right)^2}. \quad (6)$$

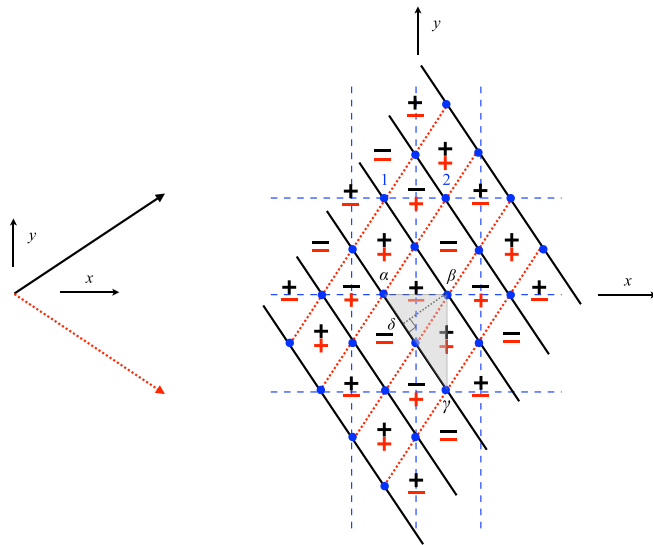


Fig. 4. Left panel: directions of non-orthogonal quasi-1D waves. Right panel: superposition of non-orthogonal standing waves on a two-dimensional membrane. The blue dashed lines are lines of zero deviation for the 2D standing-wave oscillations, locations where we can impose fixed boundaries. (See Fig. 5 for an enlarged version of the highlighted gray triangle.)

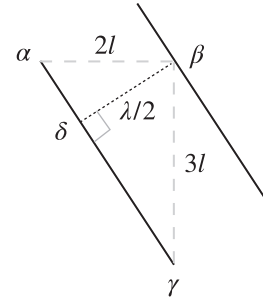


Fig. 5. Geometry of 2D standing waves for the non-orthogonal quasi-1D waves. (This is the highlighted gray triangle in the right-hand panel of Fig. 4.)

While we have used the specific 2:3 geometry for definiteness in our figures, it should be clear that the arguments apply just as well to any value of $a:b$ describing the propagation direction of the traveling waves. The generalization of (6) is

$$\frac{1}{(\lambda/2)} = \sqrt{\left(\frac{1}{al}\right)^2 + \left(\frac{1}{bl}\right)^2}. \quad (7)$$

As before, the edge lengths L_x and L_y for a rectangular membrane with fixed boundaries must be $2l$ (generally al) times some integer n and $3l$ (generally bl) times some integer m . Eliminating al and bl in (7) in favor of L_x/n , L_y/m , we can conclude that

$$f = \frac{v}{\lambda} = \frac{v}{2} \sqrt{\left(\frac{n}{L_x}\right)^2 + \left(\frac{m}{L_y}\right)^2}, \quad (8)$$

which again recovers (4) but this time for the general case of non-orthogonal quasi-1D standing waves.

To aid with visualization, we have produced animations showing the various traveling and standing-wave patterns for two different cases: (i) a square membrane ($L_x/L_y = 1$) with $n = 1$, $m = 1$ and (ii) a rectangular membrane ($L_x/L_y = 2$) with $n = 3$, $m = 2$. (See Fig. 6 for snapshots of the standing-wave oscillations.) The animations and the Matlab¹⁷ script that produced them can be found in the supplementary material.¹⁸

V. DISCUSSION

The presentation in this paper is our approach for obtaining the frequencies of standing-wave oscillations on a rectangular membrane using only algebra and basic geometry. It generalizes the explanation of standing waves on a 1D string by considering the superposition of two pairs of oppositely directed quasi-1D traveling waves to first get quasi-1D standing waves, which then combine to yield the final 2D standing-wave oscillations. The approach that we have taken here, the boundary-last approach, starts by specifying the directions and wavelength of the traveling waves and then finds the locations of the zero-deviation lines, where we can place fixed boundaries of a rectangular membrane. However, we can easily turn the argument around and apply it to the cases where the edge lengths L_x , L_y and mode numbers n , m are given *a priori*, and we are to determine the frequencies of standing-wave oscillations fixed at the boundary. We obtain the standard results for the standing-wave frequencies (4) with minimal math, sidestepping the more mathematical standard analyses, such as separation of variables. Of course,

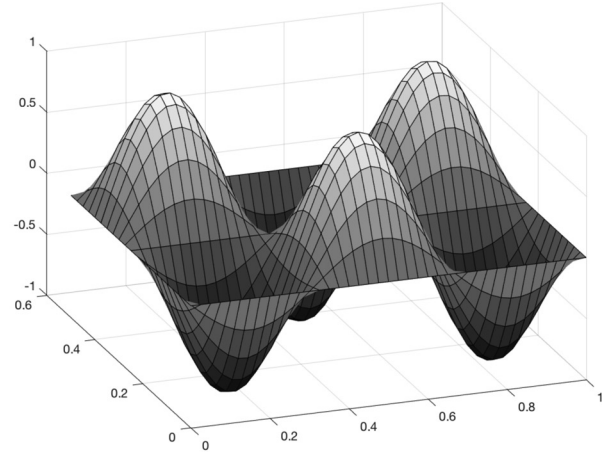
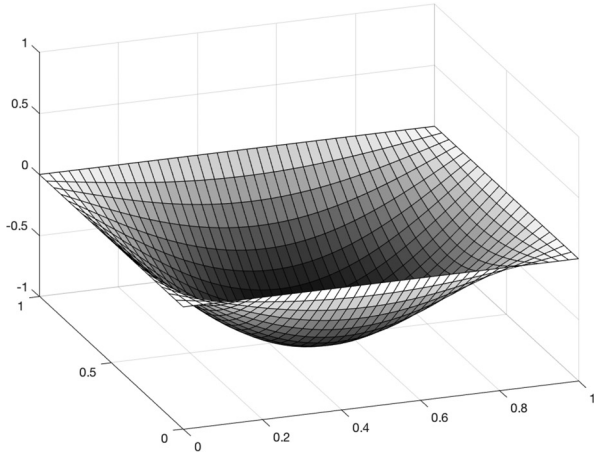


Fig. 6. Snapshots of standing wave oscillations. Left: square membrane ($L_x/L_y = 1$) with $n = 1$, $m = 1$. Right: rectangular membrane ($L_x/L_y = 2$) with $n = 3$, $m = 2$. The actual animations can be found in the supplementary material (Ref. 18).

all our constructions can be interpreted in terms of more mathematical approaches. Details relating our approach to those can be found in the [Appendixes](#).

ACKNOWLEDGMENTS

J.D.R. acknowledges fruitful discussions with Stefan Estreicher and especially Walter Borst, who had originally asked for a simple explanation of standing-wave frequencies in two and three dimensions. J.D.R. also acknowledges the support of start-up funds from Texas Tech University.

APPENDIX A: STANDARD APPROACH—SEPARATION OF VARIABLES

The standard approach for obtaining the frequencies (4) for standing-wave oscillations on a rectangular membrane fixed at the boundaries is to solve the 2D wave equation,

$$-\frac{1}{v^2} \frac{\partial^2 u}{\partial t^2} + \frac{\partial^2 u}{\partial x^2} + \frac{\partial^2 u}{\partial y^2} = 0, \quad (\text{A1})$$

for the displacement $u(t, x, y)$ of the membrane using separation of variables.^{15,16} One starts by assuming a product solution of the form $u(t, x, y) \equiv T(t)X(x)Y(y)$, for which (A1) can be written as

$$-\frac{1}{v^2} \frac{T''(t)}{T(t)} + \frac{X''(x)}{X(x)} + \frac{Y''(y)}{Y(y)} = 0. \quad (\text{A2})$$

Since the above equation is a sum of functions of t , x , and y separately, we can introduce separation constants k , k_x , and k_y defined by

$$-\frac{1}{v^2} \frac{T''(t)}{T(t)} \equiv k^2, \quad \frac{X''(x)}{X(x)} \equiv -k_x^2, \quad \frac{Y''(y)}{Y(y)} \equiv -k_y^2, \quad (\text{A3})$$

with $k^2 = k_x^2 + k_y^2$. Imposing the boundary conditions $u(t, x, y) = 0$ for $x = 0$ and L_x and $y = 0$ and L_y , for all t , leads to

$$k_x = \frac{n\pi}{L_x}, \quad k_y = \frac{m\pi}{L_y}, \quad n, m = 1, 2, \dots \quad (\text{A4})$$

The product vk has the interpretation of an angular frequency ω , so $k^2 = k_x^2 + k_y^2$ implies

$$\omega = vk = v\sqrt{k_x^2 + k_y^2}, \quad (\text{A5})$$

leading to

$$f \equiv \frac{\omega}{2\pi} = \frac{v}{2} \sqrt{\left(\frac{n}{L_x}\right)^2 + \left(\frac{m}{L_y}\right)^2}, \quad (\text{A6})$$

which are the desired standing-wave frequencies (4).

APPENDIX B: A GRAPHICAL BOUNDARY-FIRST APPROACH

In the main text, we described the boundary-last approach, where we start by specifying the directions and wavelength of quasi-1D traveling waves and then infer the location of horizontal and vertical nodal lines where we can place fixed boundaries of a rectangular membrane. In the boundary-first approach, we are given a rectangular membrane with specified edge lengths L_x and L_y , and we are asked to find the frequencies of standing-wave oscillations that are fixed at the boundaries of the rectangle. In the latter approach, we infer the directions and wavelength of the quasi-1D traveling waves from which the standing waves are subsequently made; we don't specify the directions and wavelength *a priori*.

Just as we saw for the boundary-last approach, the solution to this problem is not unique: there are many different directions and wavelengths for the quasi-1D traveling waves that yield standing-wave oscillations fixed at the boundary. These different solutions are labeled by a pair of integers n and m , which indicate the number of oscillating sections of the membrane in the x and y directions, respectively.

The direction and wavelength of the quasi-1D waves can be determined from the values of λ_x and λ_y , which are defined in the left panel of Fig. 7. The wavelength λ can be calculated in terms of λ_x and λ_y using the following "reciprocal-space version" of Pythagorean's theorem,

$$\frac{1}{\lambda^2} = \frac{1}{\lambda_x^2} + \frac{1}{\lambda_y^2}, \quad (\text{B1})$$

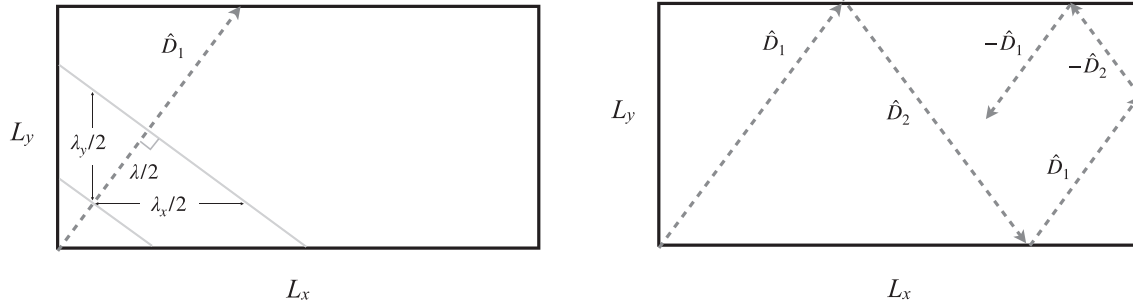


Fig. 7. Rectangular membrane with edge lengths L_x and L_y . Left: a partial set of wavefronts for the quasi-1D traveling wave with propagation direction \hat{D}_1 . The wavefronts are perpendicular to the direction of propagation and correspond here to zeros of the wave; hence, they are separated by half a wavelength, $\lambda/2$. The corresponding half-wavelengths in the x and y directions, $\lambda_x/2$ and $\lambda_y/2$, are also shown. Right: directions of propagation of the quasi-1D traveling waves reflecting off all four boundaries of the membrane.

which relates the lengths of the two sides of a right triangle to the perpendicular distance to the hypotenuse. (One can prove (B1) using similar triangles as we did in the main text in the context of Fig. 5.) From Fig. 7, we also see that the slope of the wavefronts is given by $-\lambda_y/\lambda_x$, which in turn implies that the slope of the propagation direction \hat{D}_1 is λ_x/λ_y . Thus, \hat{D}_1 is proportional to (λ_y, λ_x) ; normalizing so that it has unit length leads to

$$\hat{D}_1 = \frac{1}{\sqrt{\lambda_x^2 + \lambda_y^2}} (\lambda_y, \lambda_x) \iff \hat{D}_1 = \left(\frac{\lambda_y}{\sqrt{\lambda_x^2 + \lambda_y^2}}, \frac{\lambda_x}{\sqrt{\lambda_x^2 + \lambda_y^2}} \right), \quad (\text{B2})$$

where we used (B1) to get the last equality.

From the right panel of Fig. 7, we see that the propagation directions of the quasi-1D traveling waves change due to reflections off the horizontal and vertical boundaries of the rectangular membrane. Upon reflection off a horizontal boundary, only the y -component of the propagation direction changes (its sign flips). Similarly, upon reflection off a vertical boundary, only the x -component of the propagation direction changes (again its sign will flip). Multiple reflections recover one of these four directions, which we denote as $\pm\hat{D}_1, \pm\hat{D}_2$, where $\hat{D}_2 = (\lambda/\lambda_x, -\lambda/\lambda_y)$.

To produce standing waves fixed at the boundaries of the rectangular membrane, we need to divide each of L_x and L_y into an integer number of segments, such that

$$\lambda_x/2 = L_x/n, \quad \lambda_y/2 = L_y/m, \quad n, m = 1, 2, \dots \quad (\text{B3})$$

The wavefronts connecting the midpoints of these segments are lines of zero deviation for the quasi-1D standing waves formed from the superposition of quasi-1D traveling waves propagating in the directions $\pm\hat{D}_1, \pm\hat{D}_2$ (see Fig. 8). Substituting the above expression for λ_x and λ_y into (B1), we find

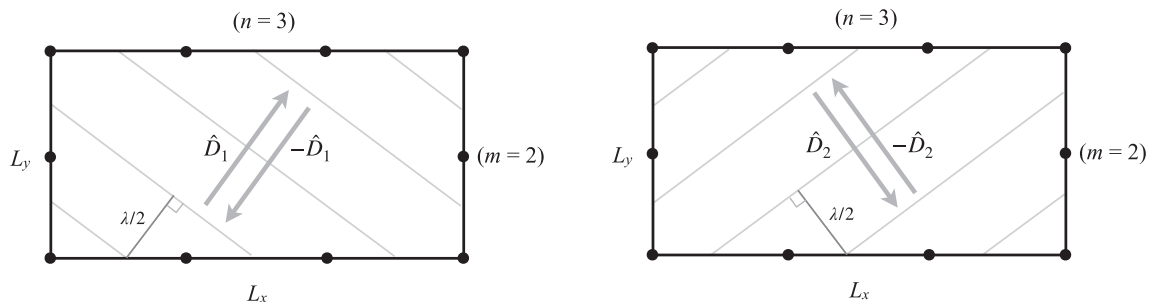


Fig. 8. Rectangular membrane with $n=3$, $m=2$. Propagation directions $\pm\hat{D}_1, \pm\hat{D}_2$, half-wavelength $\lambda/2$, and lines of zero deviation for the quasi-1D standing waves are shown.

$$\frac{1}{\lambda} = \frac{1}{2} \sqrt{\left(\frac{n}{L_x}\right)^2 + \left(\frac{m}{L_y}\right)^2}, \quad n, m = 1, 2, \dots \quad (\text{B4})$$

Then, the frequency of the waves, $f = v/\lambda$, agrees with (4).

APPENDIX C: STANDING WAVES FROM TRIG IDENTITIES

In the main text, we gave a graphical proof that the superposition of two 1D traveling waves (for a 1D string) or two quasi-1D traveling waves (for a 2D membrane) that have the same amplitude and wavelength but propagate in opposite directions gives rise to standing waves. We also gave a graphical proof that two quasi-1D standing waves with the same amplitude and wavelength can give rise to a single 2D standing wave. Here, we give an algebraic proof of these statements that makes use of a standard trig identity for the cosine of a sum (or difference) of two angles.

For the 1D string, we consider the superposition of right-moving and left-moving waves with the same amplitude and wavelength λ ,

$$u(x, t) = \cos\left[\frac{2\pi}{\lambda}(x - vt)\right] - \cos\left[\frac{2\pi}{\lambda}(x + vt)\right], \quad (\text{C1})$$

where the minus sign comes from the inversion of a right-moving wave when it is reflected off the right-most end of a fixed string. Using the trig identity,

$$\cos(A \pm B) = \cos A \cos B \mp \sin A \sin B, \quad (\text{C2})$$

with $A \equiv 2\pi x/\lambda$ and $B \equiv 2\pi vt/\lambda = 2\pi ft$, it follows that

$$u(x, t) = 2 \sin(2\pi x/\lambda) \sin(2\pi ft). \quad (\text{C3})$$

This is a standing-wave oscillation since the time-dependent term has factored out. Note that in order for the displacement $u(x, t)$ to be zero at the endpoints of the string (i.e., at $x = 0, L$) for all t , we need

$$2\pi L/\lambda = n\pi, \quad n = 1, 2, \dots \quad (\text{C4})$$

When solved for λ , this yields (3) as before and similarly the standing-wave frequencies (1).

For the 2D rectangular membrane, we have four quasi-1D traveling waves instead of two, taking into account the reflections off all the fixed boundaries. From the right panel of Fig. 7, we see that the traveling waves propagating in the $\pm\hat{D}_2$ directions are obtained from the initial \hat{D}_1 wave after an *odd* number of reflections off the boundaries. Subsequent $\pm\hat{D}_1$ waves are obtained after an *even* number of reflections. Since each reflection introduces a 180° phase shift in the wave (i.e., a minus sign), the superposition of the two-dimensional traveling waves has the form

$$\begin{aligned} u(x, y, t) = & \cos\left[\frac{2\pi}{\lambda}(\hat{D}_1 \cdot \vec{r} - vt)\right] \\ & + \cos\left[\frac{2\pi}{\lambda}(-\hat{D}_1 \cdot \vec{r} - vt)\right] \\ & - \cos\left[\frac{2\pi}{\lambda}(\hat{D}_2 \cdot \vec{r} - vt)\right] \\ & - \cos\left[\frac{2\pi}{\lambda}(-\hat{D}_2 \cdot \vec{r} - vt)\right]. \end{aligned} \quad (\text{C5})$$

Here,

$$\hat{D}_1 \cdot \vec{r} = \lambda\left(\frac{x}{\lambda_x} + \frac{y}{\lambda_y}\right), \quad \hat{D}_2 \cdot \vec{r} = \lambda\left(\frac{x}{\lambda_x} - \frac{y}{\lambda_y}\right) \quad (\text{C6})$$

are equations for the wavefronts perpendicular to \hat{D}_1 and \hat{D}_2 (relative to the bottom-left corner of the rectangular membrane, $x = 0, y = 0$), and $v/\lambda = f$ is the frequency of the waves.

Using $\cos(-\theta) = \cos \theta$ and the trig identity (C2), it follows that

$$\begin{aligned} u(x, y, t) = & 2\left\{\cos\left[2\pi\left(\frac{x}{\lambda_x} + \frac{y}{\lambda_y}\right)\right] \right. \\ & \left. - \cos\left[2\pi\left(\frac{x}{\lambda_x} - \frac{y}{\lambda_y}\right)\right]\right\} \cos(2\pi ft). \end{aligned} \quad (\text{C7})$$

Note that each of the two terms on the right-hand side of the above expression is a quasi-1D standing wave since the time-dependent term has again factored out. Using (C2) once more, we obtain

$$u(x, y, t) = -4 \sin\left(\frac{2\pi x}{\lambda_x}\right) \sin\left(\frac{2\pi y}{\lambda_y}\right) \cos(2\pi ft), \quad (\text{C8})$$

which is now a single 2D standing wave. The condition that this standing wave vanishes everywhere on the boundaries ($x = 0, L_x$ and $y = 0, L_y$) for all t implies that the arguments of the individual sine functions must be integer multiples of π , which is equivalent to (B3). Since these values for λ_x and λ_y agree with what we found earlier, so too do the expressions for the wavelength λ , cf. (B4), and frequency $f = v/\lambda$, cf. (4). So, we have again recovered the standing-wave frequencies for a rectangular membrane and the standard product-solution form for the standing waves.

^aElectronic mail: joseph.d.romano@ttu.edu

^bElectronic mail: rprice.physics@gmail.com

¹W. J. Jackson and F. R. Pratt, "A mechanical vibrator for demonstrating standing waves," *Am. J. Phys.* **4**, 205 (1936).

²M. J. Pryor, "An apparatus for demonstrating standing waves," *Am. J. Phys.* **13**, 110–111 (1945).

³E. F. Tubbs, "A machine for demonstrating standing waves," *Am. J. Phys.* **15**, 513–514 (1947).

⁴A. Hapka, "Handheld standing-wave generator," *Phys. Teach.* **38**, 342 (2000).

⁵F. P. Clay, Jr. and R. L. Kernell, "Standing waves in a string driven by loudspeakers and signal generators," *Am. J. Phys.* **50**, 910–912 (1982).

⁶A. Cortel, "Simple excitation of standing waves in rubber bands and membranes," *Phys. Teach.* **42**, 239–240 (2004).

⁷A. Crockett and W. Rueckner, "Visualizing sound waves with schlieren optics featured," *Am. J. Phys.* **86**, 870–876 (2018).

⁸G. W. Baxter and K. M. Hagenbuch, "A student project on wind chimes. Tuning in to standing waves," *Phys. Teach.* **36**, 204–208 (1998).

⁹Y. Kraftmakher, "Standing sound waves in air with DataStudio," *Phys. Teach.* **48**, 122–123 (2010).

¹⁰J. Rekveld, "On the teaching of standing waves," *Am. J. Phys.* **26**, 159–163 (1958).

¹¹R. Sorri, A. V. Baez, and Encyclopedia Britannica Educational Corporation Reviewed by J. Trusty, Reviewed by E. Ferretti, Reviewed by B. Mulligan, Reviewed by N. Stanton, and Reviewed by K. Tanaka, "Standing waves and the principle of superposition," *Am. J. Phys.* **41**, 153 (1973).

¹²M. C. LoPresto, "Experimenting with guitar strings," *Phys. Teach.* **44**, 509–511 (2006).

¹³F. W. Inman, "A standing-wave experiment with a guitar," *Phys. Teach.* **44**, 465–468 (2006).

¹⁴P. Perov, W. Johnson, and N. Perova-Mello, "The physics of guitar string vibrations," *Am. J. Phys.* **84**, 38–43 (2016).

¹⁵M. L. Boas, *Mathematical Methods in the Physical Sciences*, 3rd ed. (Wiley, Hoboken, 2006), p. 622.

¹⁶N. H. Fletcher and T. D. Rossing, *The Physics of Musical Instruments*, 2nd ed. (Springer, New York, 2010), Sec. 3.1.

¹⁷*MATLAB 2019a* (The MathWorks, Inc., Natick, MA, USA, 2019).

¹⁸See supplementary material at <https://doi.org/10.1119/10.0001299> for animations and the Matlab scripts that produced them.